Environ Sci Pollut Res (2017) 24:2578–2588
DOI 10.1007/s11356-016-7995-0

RESEARCH ARTICLE

Comparison of four methods for spatial interpolation of estimated atmospheric nitrogen deposition in South China

Linglu Qu[1,2] · **Huayun Xiao**[1] · **Nengjian Zheng**[1,2] · **Zhongyi Zhang**[1,2] · **Yu Xu**[1,2]

Received: 1 April 2016 / Accepted: 25 October 2016 / Published online: 8 November 2016

Abstract Spatial interpolation methods have been applied in many environmental research studies. However, it is still a controversial issue to select an appropriate interpolation method for the conversion of discrete sampling sites into continuous maps. This study aimed at selecting an optimal interpolation method to analyze the spatial pattern of atmospheric N deposition in South China. N deposition was calculated by 259 moss sample data. Four spatial interpolation methods, including inverse distance weighting (IDW), radial basis function (RBF), ordinary kriging (OK), and universal kriging (UK), were utilized for modeling the spatial distribution of N deposition. It is the first time that these methods were applied to analyze N deposition in South China. Validation method was used to evaluate the interpolation precision of the various methods, and the cross-validation method was used to evaluate their interpolation accuracy. Comparison of predicted values with measured values indicated that OK was the optimal method for analyzing the spatial distribution of N deposition in this study; it had the highest precision (mean error (ME) = −0.059, root-mean-square error (RMSE) = 5.240, mean relative error (MRE) = 0.129, mean absolute error (MAE) = 4.007) and the lowest uncertainties (standard deviation (SD) = 5.47, coefficient of variation (CV) = 0.15). RBF produced similar results as good as OK, while the worst performed interpolation method was UK. By using the OK method for analyzing N deposition, this work revealed systematic temporal and spatial variations in atmospheric N deposition in South China.

Keywords Estimated N deposition · Moss biomonitoring · Spatial distribution · Interpolation · Cross-validation

Responsible editor: Gerhard Lammel

✉ Huayun Xiao
xiaohuayun@vip.skleg.cn

[1] State Key Laboratory of Environmental Geochemistry, Institute of Geochemistry, Chinese Academy of Science, Guiyang 550081, China

[2] University of Chinese Academy of Sciences, Beijing 100049, China

Introduction

Atmospheric N deposition is an important part of global biogeochemical N cycle (Goulding 1990). Intensive anthropogenic activities have greatly increased the concentration of reactive nitrogen into the environment and have large impacts on the composition and source of N deposition (Galloway et al. 2004; Huang et al. 2015; Liu et al. 2015; Lu et al. 2015). A large number of studies have revealed a rapid increase in atmospheric N deposition in China, with the deposition centered in the southeast (Chen and Mulder 2007; Huang et al. 2010; Huang et al. 2013; Jia et al. 2014; Lü and Tian 2014). It is well documented that the excess of N deposition has a severe adverse effect on sensitive ecosystems and human health (Bouwman et al. 2002; Clark and Tilman 2008; Liu et al. 2011; Nyberg et al. 2000; Schwartz 1994). For the purpose of integrated nutrient management and evaluation of the ecological environmental effect of N deposition, therefore, it is necessary to investigate the source, quantity, and temporal-spatial distribution of atmospheric N deposition. The spatial information is of great significance for the research of N deposition in different scales. At present, massive papers have reported the deposition of atmospheric nitrogen on a global, regional, or local scale (Cui et al. 2014; Fenn et al. 2003; Galloway and Cowling 2002; Galloway et al. 2008; Lü and Tian 2014; Nadim et al. 2001; Pan et al. 2012). There are still some problems on the study of N deposition, including (a) the number of monitoring sites is

unevenly distributed and insufficient; (b) monitoring focus on wet deposition, either dry deposition and fog deposition are not measured or only partially quantified; and (c) technical difficulties and high costs are still challenges for measuring the atmospheric concentrations and deposition (Chang et al. 2013; Fenn et al. 2003). Thus, interpolation methods are used in mapping N deposition pollution.

Spatial interpolation methods are divided into the following two main categories: deterministic interpolation methods, such as inverse distance weighting, and geostatistical interpolation methods, such as kriging (Cressie 1992). In a geographic information system (GIS), spatial interpolation methods are very powerful tools for predicting the values of an attribute at unsampled sites in order to generate spatially continuous data (Atkinson 2005; Li and Heap 2011). In spite of their development for over 50 years, spatial interpolation methods are mainly used for the analysis of precipitation, meteorological factors, and soil elements. With the advances of computer technology, GIS capabilities for spatial interpolation have improved. In recent years, spatial interpolation methods integrated with GIS are used for simulation of the spatial distribution of atmospheric N deposition (Jia et al. 2014; Lü and Tian 2007, 2014; Zhu et al. 2015). There are a lot of studies on comparison of spatial interpolation methods for different objectives, but the results are not conclusive. Some papers reported that kriging outperformed other methods (Sun et al. 2009; Zhong 2010; Zimmerman et al. 1999), while in others, inverse distance weighting or radial basis function was as good or better (Laslett et al. 1987; Lu and Wong 2008; Weber and Englund 1992). And, there have been few reports comparing different interpolation methods for N deposition in China.

In view of the significant correlation between moss N content and atmospheric N deposition even at low levels, moss N content is widely used to substitute direct measurements of N deposition at locations without instrumental monitoring (Liu et al. 2008a; Skinner et al. 2006). According to some previous data, Liu et al. (2009) summarized an integrated relationship between N deposition and tissue N contents in mosses and assessed the level of atmospheric N deposition in Guiyang. This good linear pattern was also successfully applied to the estimation of atmospheric N deposition in the Yangtze River drainage basin (Xiao et al. 2010b). Therefore, moss N content was used to estimate atmospheric N deposition in this study. The moss method also proved useful to assess the spatial distribution of N deposition (Pesch et al. 2007; Skudnik et al. 2016; Varela et al. 2013).

Considering the importance of spatial variation of atmospheric N deposition, this study was undertaken to compare the performance of four types of representative interpolation methods, including inverse distance weighting (IDW), radial basis function (RBF), ordinary kriging (OK), and universal kriging (UK), by cross-validation and validation methods. Then, a relatively appropriate interpolation method was selected to explore the spatial distribution of estimated N deposition in South China.

Data and analysis

Data sources

We collected the same moss as Xiao et al. (2010b) reported in Yunnan, Guizhou (except Guiyang, Anshun, and Zunyi cities), and Anhui provinces from 2011 to 2013. All sampling sites (259) were located in open habitats. All samples were collected from natural rocks above ground level to avoid the influence of surface water splashes, overlapping by canopies and buildings, and other anthropogenic pollution. If mosses were collected around urban parks or hills, the sampling sites were located at least 500 m from main roads and at least 100 m from other roads or houses. At each sampling site, 5–10 subsamples were collected and combined into 1 representative sample. After rinsing with 1.5 mol/L HCl, washing with deionized water, and sonicating several times, all fresh samples were dried in a vacuum oven at 70 °C and then were separately ground into fine powders. Moss N concentrations were measured by an elemental analyzer (Model PE-2400 II, PerkinElmer, USA) with an analytical precision of 1%. We used the oatmeal standard (AR 2026) from Alpha Resources Inc., USA (+1.83%), for our analysis, which gave a mean (±standard deviation (SD)) N% value of 1.83 ± 0.01%. Moss data in other regions, including Sichuan, Hunan, Hubei, Guangzhou, Guangxi, Fujian, Zhejiang, Jiangsu, and Jiangxi provinces; Chongqing and Shanghai municipalities; and Guiyang, Anshun, and Zunyi cities, were summarized from published sources for the 2006–2009 period (Liu et al. 2008b; Xiao et al. 2010a, b, 2011). The mean N deposition (y) was calculated per site by tissue N contents of moss (x), and the relevant equation is (Xiao et al. 2010b)

$$y = 19.23x - 14.04 \quad (1)$$

The data used in this study were placed in Geostatistical Analyst of ArcGIS with a grid resolution of 6 × 6 km. Two-hundred and fifty-nine sampling sites, which are shown in Fig. 1, covered the whole of South China, including 14 provinces (municipalities and autonomous regions).

Data exploration

The Explore Data tool of ArcGIS 10.2 (ESRI 2011) and SPSS 19.0 software (SPSS Inc., Chicago, IL, USA) were employed to conduct data analyses, including the data's distribution, outlier identification, and trend analysis. In Fig. 2a, the normal quantile-quantile plot (normal QQ plot) showed that the estimated N deposition data tended to follow a normal

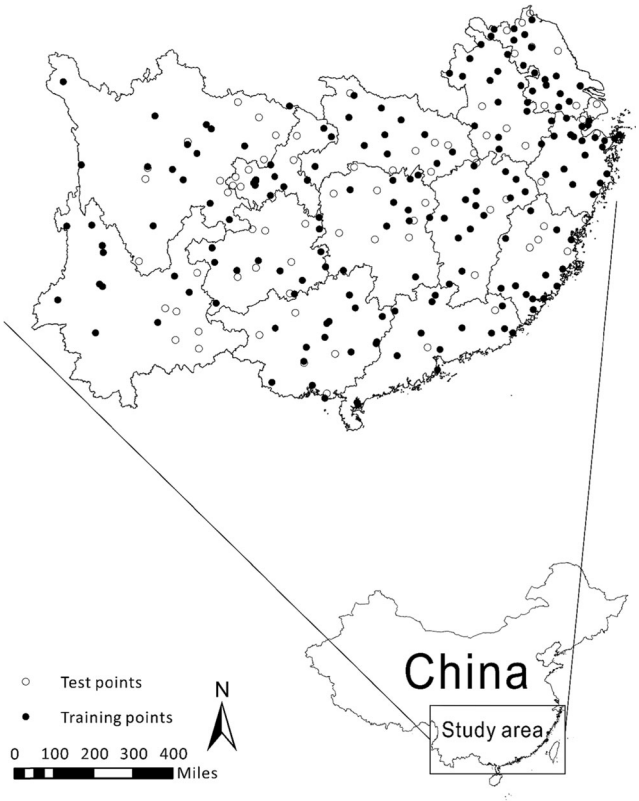

Fig. 1 Distribution of sampling points in South China

distribution. The normal distribution test and normal distribution plot, which are shown in Table 1 and Fig. 2b, also revealed the same result.

Outliers can have several detrimental effects on the prediction surface because of effects on semivariogram modeling and the influence of neighboring values (ESRI 2011). Voronoi maps based on the cluster and entropy methods were used to identify possible outliers. Because the estimated value of one sampling point was unusually higher than that of the surrounding points, it was removed before creating a surface.

Trend analysis is essential for data exploration. It can directly reflect the total change trend of spatial data. From the trend analysis plot (Fig. 2c), we found that the spatial correlation of the estimated data was strong. It showed that N deposition gradually increased from the northwest to the southeast, while the change trend was parabola in shape from the southwest to the northeast. So, it was clear that there was spatially significant difference in N deposition in South China, and its spatial variation presented a quadratic trend.

Spatial autocorrelation analysis

Spatial autocorrelation analysis was carried out on the estimated N deposition data before interpolation. It is a method of spatial statistics which can reveal the spatial structure of regional variables. In general, spatial autocorrelation analysis is used for quantitative description of interdependent relationship between each of the variables in space. If similar values are spatially close to each other, they are correlative; otherwise, they are independent or randomly distributed in space. The similarity of spatial variables is decided by Moran's *I*. Its value ranges from −1 to 1. Similar values in space cluster

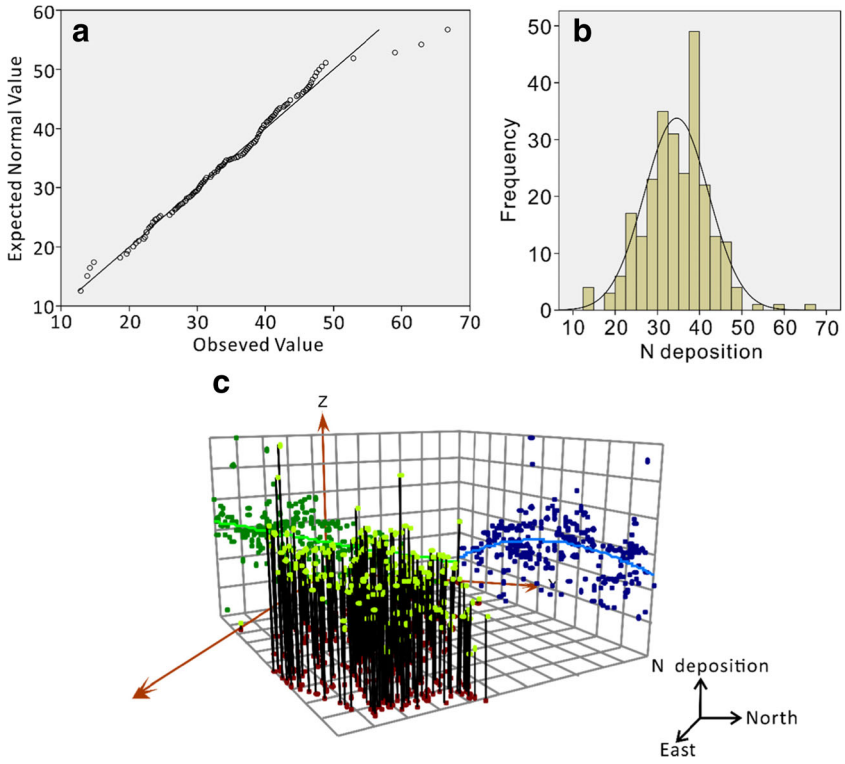

Fig. 2 Data analysis test of nitrogen deposition of sampling points. **a** Normal QQ plot, **b** normal distribution plot, and **c** trend analysis plot

Table 1 Tests of normality by one-sample Kolmogorov-Smirnov test

		N deposition
N		258
Normal parameters[a, b]	Mean	34.5346
	Standard deviation	7.6444
Most extreme differences	Absolute	0.065
	Positive	0.041
	Negative	−0.065
Kolmogorov-Smirnov *Z*		1.042
Asymp. Sig. (two-tailed)		0.228

[a] Test distribution is normal

[b] Calculated from data

together when Moran's *I* is close to 1, while dissimilar values cluster together when Moran's *I* is close to −1. Values in space are irrelevant when Moran's *I* is close to 0 (Moran 1948). The Moran's *I* index was 0.66, which was calculated by the method of inverse distance-weighted Euclidean distance. It implied that the data of N deposition was highly spatially autocorrelative.

Geostatistical method

Semivariogram

Semivariogram is used to describe the randomness and structuredness of regional variables. It is a quantitative index applied to characterize the autocorrelation of spatial data, with the following expression (Cressie 1992):

$$\gamma(h) = \frac{1}{2N(h)} \sum_{i=1}^{N(h)} [Z(x_i) - Z(x_i + h)]^2 \quad (2)$$

where $\gamma(h)$ is the semivariogram, h is the delay distance or step size, $N(h)$ is the number of point pairs with a distance of h, and $Z(x_i)$ and $Z(x_i + h)$ are the measured values of $Z(x)$ in locations x_i and $x_i + h$, respectively.

A variety of standard functions is used in semivariogram modeling. It is a critical step of the transformation from spatial description to spatial prediction. However, the results were distinct when different models were used for spatial interpolation (Zhang et al. 2013). For the sake of high precision, repeated comparisons should be conducted to select an optimal model in the process of fitting semivariogram.

Spatial interpolation methods

A geostatistical analysis program in ArcGIS 10.2 was used to interpolate the spatial data (ESRI 2011). A comparison of four spatial interpolation methods was conducted to select an optimal method.

Inverse distance weighting

The IDW method is one of the simplest and most common interpolation methods. It is based on a similar principle that the properties of two points are similar when they get close in space or vice versa. It makes the distance between interpolation sites and sampling sites as weights and takes a weighted average estimation for the values of unsampled sites. Higher weighting values will be assigned to those points which are closer to the interpolation point (Isaaks and Srivastava 1989). Formally, the estimation of unknown values is in the following manner:

$$Z(s_0) = \sum_{i=1}^{N} \lambda_i Z(s_i) \quad (3)$$

where $Z(s_0)$ is the estimated value in location s_0, N is the number of sampling sites around predicted sites, λ_i is the weight which is usually inversely proportional to the distance between sampling sites and predicted sites, and $Z(s_i)$ is the measured value in location s_i.

The weight formula can be given as

$$\lambda_i = d_{i0}^{-p} \Big/ \sum_{i=1}^{N} d_{i0}^{-p}, \quad \sum_{i=1}^{N} \lambda_i = 1 \quad (4)$$

where d_{i0} is the distance between s_0 and s_i and p is an exponent usually set to 2. With the increase of the distance between sampling sites and predicted sites, the weight declines exponentially. The weights assigned to the predicted sites are proportional, and they are made to sum to 1.

Radial basis function

The RBF method is an exact interpolation method; namely, the interpolation surface must go through every known point. It is a monotone function of Euclidean distance between a certain point X and a center point X_0. RBF is applied to interpolate a large number of data points so as to generate a smooth surface (Powell 1990). The estimator is as follows:

$$Z(s_0) = \sum_{i=1}^{N} Z(s_i) G(d_{i0}) \Big/ \sum_{i=1}^{N} G(d_{i0}) \quad (5)$$

where $G(d_{i0})$ is the monotone function of Euclidean distance; other parameters are the same as the abovementioned parameters.

Ordinary kriging

OK is one of the most common kriging interpolation methods. It provides an unbiased estimate for variables in regions where the available data are spatially autocorrelative. On the premise

of meeting the intrinsic hypothesis, its estimator is the same as IDW. The only difference is that a semivariogram is used to determine the weight (Cressie 1990).

Universal kriging

The OK method proposes an assumption that regional variables meet second-order stationary hypothesis. However, the assumption is not consistent with the actual situation sometimes. In the presence of a drift, a new optimal linear estimation method is used for spatial interpolation. The UK method assumes that the available data exhibit a dominant trend and the trend can be fitted by a certain function or polynomial. We need to analyze the change trend of the data, firstly, in order to get a simulated model. Then, a kriging method is conducted to analyze the residual data. Finally, the results of trend-surface and residual analysis are summed to generate a final result (Matheron 1969).

Comparison of the precision and accuracy of interpolation methods

Validation method was used to evaluate the precision of different interpolation methods in this study. Two subsets were constructed for 258 data by the Geostatistical Analyst tool in ArcGIS 10.2. The Create Subset tool was used to specify the size of training subset. We changed the default percentage of training and test subsets, which are 50 and 50%, respectively, based on the previous experience. As shown in Fig. 1, 70% of the sampling sites (N = 181) were separated out as training subsets (also known as training points) and the remaining 30% (N = 77) were as test subsets (also known as test points). Training subsets were used to model the spatial structure and produce a surface. Values of the other 79 sampling sites removed were estimated via abovementioned four interpolation methods based on the other surrounding sites. Then, a correlation analysis was made for predicted values and estimated values so as to assess the precision of spatial interpolation methods. Commonly used evaluation indicators include Pearson's correlation (R), mean error (ME), mean relative error (MRE), mean absolute error (MAE), and root-mean-square error (RMSE). These indices take the form

$$R = \frac{1}{n-1}\sum_{i=1}^{n}\left(\frac{x_i-\overline{x}}{S_x}\right)\left(\frac{y_i-\overline{y}}{S_y}\right) \tag{6}$$

$$\mathrm{ME} = \frac{1}{n}\sum_{i=1}^{n}\left(p_i-o_i\right) \tag{7}$$

$$\mathrm{MRE} = \frac{1}{n}\sum_{i=1}^{n}\left|\frac{o_i-p_i}{o_i}\right| \tag{8}$$

$$\mathrm{MAE} = \frac{1}{n}\sum_{i=1}^{n}\left|p_i-o_i\right| \tag{9}$$

$$\mathrm{RMSE} = \left[\frac{1}{n}\sum_{i=1}^{n}\left(p_i-o_i\right)^2\right]^{1/2} \tag{10}$$

In Eq. (6), $\frac{x_i-\overline{x}}{S_x}$, $\overline{x}$, and S_x represent the standardized variable, sample mean, and sample standard deviation, respectively. In Eqs. (7), (8), (9), and (10), n is the number of sampling sites, o_i is the estimated values, and p_i is the predicted values.

ME reflects the degree of overall estimation bias. MRE is used to determine the accuracy of predicted values compared with estimated values. MAE and RMSE are the best measure indicators for interpolation precision. A high MAE suggests that an interpolation method does a poor job in prediction, while RMSE provides a measure of error size. Although RMSE and MAE are similar measure indicators, RMSE is more sensitive to extreme values than MAE (Li and Heap 2011). The evaluation standard is that the lower ME, MRE, MAE, and RMSE of interpolation results are, the higher interpolation precision will be.

Cross-validation is a commonly used method for comparing the accuracy of interpolation methods. Every sampling site is individually removed, and its value is estimated by the other surrounding sites. This process continues until values of all sampling sites are estimated (Stone 1974). Two commonly used indicators for evaluating uncertainties of interpolation methods are coefficient of variation (CV) and SD. CV is a normalized indicator of dispersion tendency, while SD is used to indicate dispersion tendency of results (Mirzaei and Sakizadeh 2016). Smaller CV and SD values indicate less uncertainty of interpolation methods.

$$\mathrm{CV} = \sqrt{\frac{\sum_{i=1}^{n}\left(x_i-\overline{x}\right)^2}{n-1}}\Big/\overline{x} \tag{11}$$

$$\mathrm{SD} = \sqrt{\frac{\sum_{i=1}^{n}\left(x_i-\overline{x}\right)^2}{n-1}} \tag{12}$$

In Eqs. (11) and (12), all parameters are the same as above.

Results

Selection of semivariogram models

For two, in the study used, kriging methods (OK and UK), it is essential to select an optimal semivatiogram model for data analysis. In this paper, a cross-validation analysis was

implemented to evaluate the precision of kriging semivariogram models. The linear regression analysis method was used to make a comparison between estimated values and predicted values, and then, an optimal semivariogram model was selected (Wu and Yan 2007). The selection criteria are as follows: (a) the lower the standard error (SE) of regression coefficient is, the higher the precision of model simulation will be; (b) the higher the correlation coefficient (R^2) is, the better the regression effect of simulation results will be; and (c) the lower the predicted value of standard error (SE prediction) is, the smaller the prediction error of models will be. Table 2 shows the precision cross-validation results of five models, including spherical, exponential, Gaussian, hole effect, and J-Bessel models. In the OK method, all cross-validation indicators of five models showed little change. The SE and SE prediction for the hole effect model had the smallest values (0.035 and 1.238), and the R^2 for hole effect model has the largest (0.510). Therefore, the hole effect model (nugget 23; sill 21; and practical range 529,656 m) was the optimal theoretical semivariance function for the OK method. On the contrary, the SE, R^2, and SE prediction values of the five models for the UK method ranged from 0.041 to 0.094, 0.007 to 0.523, and 1.437 to 24.355, respectively. The SE and SE prediction for the J-Bessel model had the smallest values (0.041 and 1.437), and the R^2 value was the largest (0.523). It was clear that the J-Bessel model (nugget 16; sill 30; and practical range 529,656 m) was optimal for the UK method.

Precision and accuracy of different interpolation methods

Table 3 shows that predicted values estimated by different interpolation methods were significantly related to estimated values, and the R for IDW was the largest (0.728). The ME, which measured the bias, showed that bias was very small (near zero) for the OK (−0.059) method, whereas the UK method (−2.963) had comparatively more bias. MRE provides a measure of interpolation accuracy, with lower values indicating more accurate methods. The difference in MRE for the IDW, RBF, and OK methods was very small, with the minimum of 0.129 for OK, while UK had the largest MRE (2.402). Therefore, OK was more accurate than the other methods. RMSE and MAE are two similar measure indicators for interpolation precision. The interpolation of atmospheric N deposition data resulted in RMSE and MAE between 5.240 and 9.707 and 4.007 and 6.685, respectively. The highest precision was obtained by OK (RMSE = 5.240, MAE = 4.007). The RBF method performed nearly as well as OK. Among the different methods, UK interpolation had the largest error. As a whole, taking all the indicators into consideration, the OK method showed the best performance than the other methods, although the RBF method also produced similarly good results.

Table 3 Results of precision and correlation test for different interpolation methods

	ME	RMSE	MRE	MAE	R	Significance
IDW	1.422	6.443	0.145	4.621	0.728	0.000**
RBF	0.346	5.295	0.136	4.084	0.714	0.000**
OK	−0.059	5.240	0.129	4.007	0.628	0.000**
UK	−2.963	9.707	2.402	6.685	0.327	0.003*

*$P < 0.01$ indicates that predicted values are significantly correlated with measured values

**$P < 0.001$ indicates that predicted values are highly, significantly correlated with measured values

The values of SD and CV for all different interpolation methods fluctuated between 5.47 and 7.17 and 0.15 and 0.21 (Table 4). The first three methods had similar prediction accuracy. SD and CV values of 7.17 and 0.21 indicated that the uncertainty of the UK method was the largest. The smallest SD and CV values were 5.47 and 0.15 for the OK method, respectively. Thus, interpolation results obtained from OK were the most accurate. This result also was supported by Fig. 3. A regression coefficient closer to 1.00 and a higher R^2 value indicate more reliable results of interpolation. As can be seen in Fig. 3, the regression coefficient and R^2 for OK (0.99 and 0.56) were higher than that for the other methods. It was clear that the

Table 2 Cross-validation for precision evaluation of semivariogram models

Model	Lag size (m)	Number of point pairs in each lag	OK			UK		
			SE	R^2	SE prediction	SE	R^2	SE prediction
Spherical	44,138	32	0.036	0.493	1.270	0.044	0.475	1.540
Exponential			0.037	0.492	1.300	0.086	0.087	3.031
Gaussian			0.036	0.470	1.286	0.094	0.228	3.332
Hole effect			0.035	0.510	1.238	0.689	0.007	24.355
J-Bessel			0.036	0.489	1.287	0.041	0.523	1.437

SE standard error of regression coefficient, R^2 correlation coefficient, *SE prediction* predicted value of standard error

Table 4 The coefficient of variation and standard deviation of cross-validation results for different interpolation methods

Method	SD	CV
IDW	5.80	0.16
RBF	5.73	0.16
OK	5.47	0.15
UK	7.17	0.21

rank of prediction accuracies for the four interpolation methods was OK > RBF > IDW > UK.

Spatial distribution of atmospheric N deposition

The spatial distribution of atmospheric N deposition in South China was interpolated in turn using the IDW method, the BRF method, and the kriging methods (OK and UK). To explore the effect of the four interpolation methods on the spatial variation of N deposition, we made a comparison for interpolation maps. All interpolation methods reflected the overall trend of N deposition (Fig. 4). Obviously, the deposition rate of atmospheric N increased from northwest to southeast. And, deposition centered in the southeastern part. As shown in Fig. 4, different surface smoothness was produced by three interpolation methods, including IDW, RBF, and OK. The IDW method resulted in obvious "bull's-eye" effect in some areas. This effect was improved by the RBF method, while the OK method generated a relatively smoother surface than the first two methods. In addition, there were no considerable differences in the spatial variation of N deposition estimated by these three methods. The deposition rate ranged between 10 and 70 kg N ha^{-1} yr^{-1}. However, the UK method had a significant influence on the estimation of N deposition. N deposition in most areas was overestimated, while serious interpolation errors appeared in the northwestern end of South China and its southwestern end with sparse sampling sites. The comparison results confirmed that the OK method can effectively avoid the system errors and was more precise than the other methods for reflecting the spatial distribution of N deposition.

Discussion

With their special physiological properties, mosses have been identified as a reliable biomonitor of N deposition (Pitcairn et al. 2006). A good linear equation, which integrated from previous reported data (Bragazza et al. 2005; Pitcairn et al. 1995, 2001; 2002; Solga et al. 2005), was used to calculate atmospheric N deposition in this study. This equation also was successfully applied in our previous study (Liu et al. 2009; Xiao et al. 2010b). The spatial variation of N deposition was then interpolated using the IDW, RBF, OK, and UK methods. Spatial interpolation methods have been widely used in various environmental research studies. Their effectiveness is related to interpolation precision and accuracy. However, most studies focus on interpolation accuracy (Gong et al. 2014;

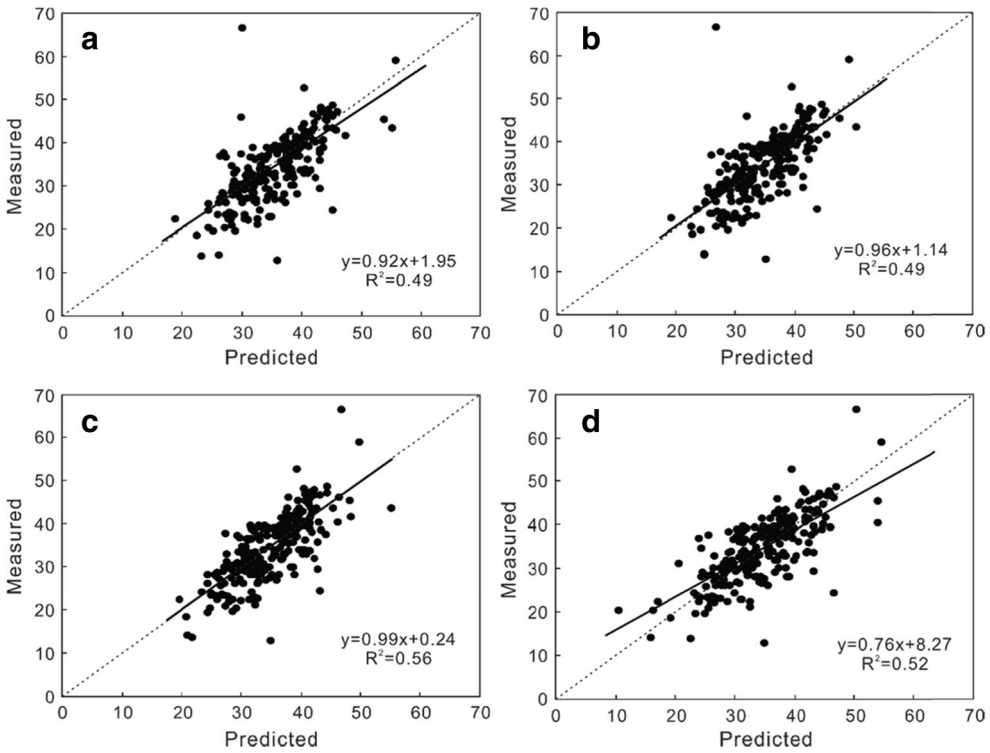

Fig. 3 The cross-validation analyses of different interpolation methods. **a** IDW, **b** RBF, **c** OK, and **d** UK

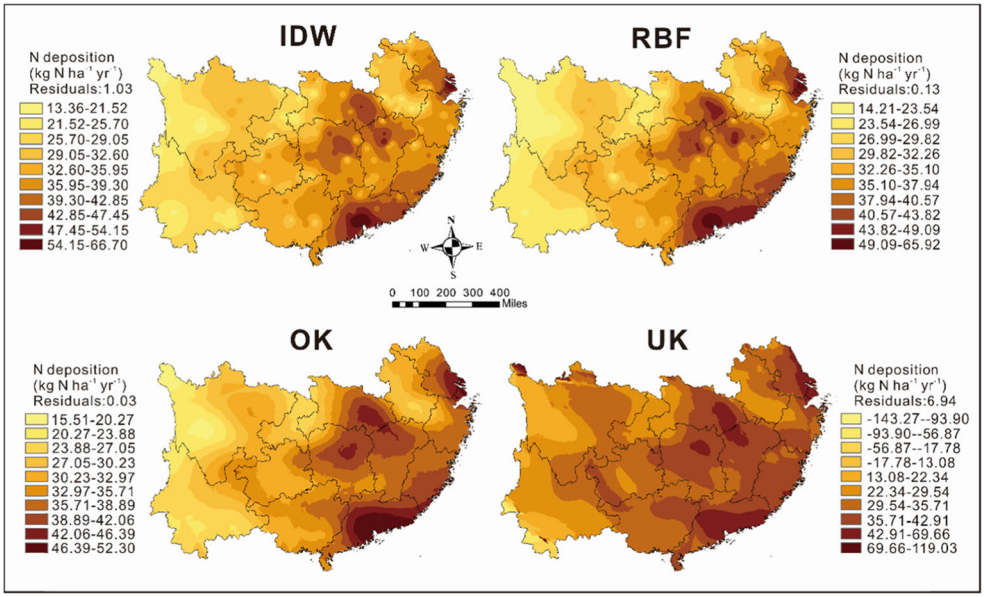

Fig. 4 Spatial patterns of atmospheric nitrogen deposition in South China (kg N ha^{-1} yr^{-1})

Lloyd 2005; Yao et al. 2013; Zimmerman et al. 1999). The present study, for the first time, compared the interpolation accuracy and precision of the common four methods.

Interpolation processes generally induce uncertainty in results (Liu et al. 2014). The main factors affecting the performance of spatial interpolation methods are the number of samples, sampling design, and the choice of interpolation methods (Kravchenko 2003; Li and Heap 2011). One of the premises of optimal interpolation method is high interpolation precision. It stated that sampling design significantly affected the performance of the methods in terms of RMSE and MAE (Li and Heap 2011). Because of irregularly spaced data, these two precision indicators in this study indicated some differences between different interpolation methods, varied from 5.240 to 9.707 and 4.007 to 6.685, respectively (Table 3). All precision indicators were lower for OK than that for other methods, although the difference between RBF and OK was small. Interpolation precision is not the unique criterion of interpolation optimality. An optimal interpolation method should also provide accurate predicted results. Cross-validation is a widely used and effective method for the evaluation of interpolation methods (Gong et al. 2014; Lloyd 2005). However, the number of monitoring sites usually introduces bias into results. Cheng et al. (2008) and Wagner et al. (2012) reported that a large bias was induced to interpolation results especially in low-density monitoring sites, unless sites were designed to meet the interpolation requirements. Limited sampling wells had an impact on the estimation of groundwater quality in the Andimeshk-Shush Plain in Iran (Mirzaei and Sakizadeh 2016). In our study, with a limited number of sampling sites in remote areas, the results were subjected to bias. SD and CV results for different interpolation methods showed that interpolation accuracy was the best for OK, while the uncertainty originated from UK was more than any other methods (Table 4).

Interpolation optimality also depends on how well the interpolation methods reflect the spatial variation of research subjects (Xie et al. 2011). The results in this study demonstrated that the choice of different interpolation methods had influence on the spatial distribution of N deposition (Fig. 4). Serious interpolation errors were produced by UK in the border, although all methods reflected the overall trend of N deposition. The smoothing effect of OK was much stronger than IDW and RBF. Xie et al. (2011) reported that some real information in a local region was likely to be smoothed out by OK. Journel et al.'s (2000) research also indicated that an optimal interpolation method should produce estimation maps with relatively low interpolation smoothing. With the purpose of analyzing the spatial distribution of N deposition, the prediction result should be as precise as possible. There was no doubt that OK had the strongest ability to predict the overall trend of N deposition in South China. What is also notable is that numerous other environmental variables (such as precipitation, altitude, and canopy drip) could influence the moss N content and then have an effect on the spatial distribution of estimated N deposition (Meyer et al. 2015; Pesch et al. 2008; Schröder et al. 2010; Skudnik et al. 2014, 2015).

Many studies have shown that model parameters have an important effect on simulation results (Liu et al. 2014; Mirzaei and Sakizadeh 2016). In general, IDW and RBF are easy to use and need less input parameters. In contrast, the kriging method needs more parameters, and its calculation process is more complex (Liu et al. 2014). Typically, kriging interpolation comprises of the following steps: statistic test, data transformation and inverse transformation, spatial structure analysis, and semivariance function fitting (Xie et al. 2011). It is

worth noting that a lot of decisions and calculation steps are done automatically by the ArcGIS software. Thus, the semivariance fitting is empirical in most cases; different researcher may have different conclusions (Xie et al. 2011). Jia et al. (2014) found that the kriging method worked well to predict the spatial patterns of N deposition in China. However, Kravchenko (2003) pointed out that kriging was as accurate as IDW when variogram parameters were determined from sample variograms but was less precise when a reliable sample could not be obtained from the data. It should be noted that the kriging methods are not optimal for all environmental research studies. In this study, the OK method provided a best linear unbiased estimation accounting for the statistical distribution of estimated N deposition data. It produced a better local accuracy in the border through minimization of a covariance-based error variance. Therefore, the more complex calculating process and more parameters might be the reason for lower uncertainty for OK. These redeeming features made it an appealing method.

It should be clear that in addition to the above impact factors, there are other factors which also affect the performance of spatial interpolation methods. Previous findings showed that when sample density was high, most methods produced similar results. When sample density is relatively low, the performance of spatial interpolation methods was better when the sample density increases (Stahl et al. 2006). The uncertainty of interpolation results might relate to the spatial autocorrelation. Samples with a strong spatial autocorrelation were mapped more accurately than samples that had weak spatial autocorrelation (Liu et al. 2014). In this study, we did not consider the characteristics of sampling areas and monitored pollutants. It is recommended that further research studies should be done when the OK method is used in the spatial analysis of atmospheric N deposition in other regions.

Conclusion

OK was the optimal method for exploring the spatial distribution of atmospheric N deposition in this study. This conclusion was based on moss data in South China in the period of 2006 and 2013, which were in turn interpolated using the IDW, RBF, OK, and UK methods. Validation was used to evaluate the interpolation precision of different methods. The results showed that OK had the highest precision (ME = −0.059, RMSE = 5.240, MRE = 0.129, MAE = 4.007). Cross-validation was then used to evaluate the interpolation accuracy. Measures of uncertainty indicated that OK had the lowest coefficient of variation (0.15) and standard deviation of estimation errors (5.47). Uncertainties of three methods (IDW, RBF, and OK) were very similar. Atmospheric N deposition in South China obviously increased from northwest to southeast. The highest deposition was located in the southeastern part. However, different interpolation methods generated different predictions in local areas. The smoothing effect of OK was stronger than that of the other methods. Serious interpolation errors, produced by UK, appeared in the northwestern and southwestern borders with sparse sampling sites. Although RBF also produced similarly good results, we would recommend the OK method to be used in this study, especially for scarce sampling site that was insufficient to fit a semivariogram model. These differences among the performance of four interpolation methods were attributed largely to three main factors, including the number of samples, sampling design, and the choice of interpolation methods. However, it should be noted that other factors, such as sample density and spatial autocorrelation, also might affect the performance of interpolation methods (Liu et al. 2014; Stahl et al. 2006). Thus, more research studies are needed to be done when the OK method is applied in estimating atmospheric N deposition.

Acknowledgments This study was kindly supported by the National Key Research and Development Program of China through grant 2016YFA0601000 (H.Y. Xiao); the National Natural Science Foundation of China through grants 41425014, 41273027, and 41173027 (H.Y. Xiao); and the National Basic Research Program of China through grant 2013CB956703 (H.Y. Xiao).

References

Atkinson PM (2005) Spatial prediction and surface modeling. Geogr Anal 37:113–123. doi:10.1111/j.1538-4632.2005.03702002.x

Bouwman AF, Van Vuuren DP, Derwent RG, Posch M (2002) A global analysis of acidification and eutrophication of terrestrial ecosystems. Water Air Soil Pollut 141:349–382. doi:10.1023/a:1021398008726

Bragazza L, Limpens J, Gerdol R, Grosvernier P, Hajek M, Hajek T, Hánsen P, Iacumin P, Kutnar L (2005) Nitrogen concentration and $\delta^{15}N$ signature of ombrotrophic *Sphagnum* mosses at different N deposition levels in Europe. Glob Chang Biol 11:106–114

Chang YH, Liu XJ, Li KH, Lv JL, Song W (2013) Numerical modeling atmospheric nitrogen deposition: evolution process and models' screening. Arid Land Geograp 36:383–392 (in Chinese)

Chen XY, Mulder J (2007) Atmospheric deposition of nitrogen at five subtropical forested sites in South China. Sci Total Environ 378: 317–330. doi:10.1016/j.scitotenv.2007.02.028

Cheng KS, Lin YC, Liou JJ (2008) Rain-gauge network evaluation and augmentation using geostatistics. Hydrol Process 22:2554–2564. doi:10.1002/hyp.6851

Clark CM, Tilman D (2008) Loss of plant species after chronic low-level nitrogen deposition to prairie grasslands. Nature 451:715

Cressie N (1990) The origins of kriging. Math Geol 22:239–252. doi:10.1007/bf00889887

Cressie N (1992) Statistics for spatial data. Terra Nov. 4:613–617

Cui J, Zhou J, Peng Y, He YQ, Yang H, Xu LJ, Chan A (2014) Long-term atmospheric wet deposition of dissolved organic nitrogen in a typical red-soil agro-ecosystem, southeastern China. Environ Sci Proc Imp 16:1050–1058. doi:10.1039/C3EM00613A

ESRI R (2011) ArcGIS desktop: release 10. Environmental Systems Research Institute, CA

Fenn ME, Haeuber R, Tonnesen GS, Baron JS, Grossman-Clarke S, Hope D, Jaffe DA, Copeland S, Geiser L, Rueth HM, Sickman JO

(2003) Nitrogen emissions, deposition, and monitoring in the western United States. Bioscience 53:391–403. doi:10.1641/0006-3568(2003)053[0391:nedami]2.0.co;2

Galloway JN, Cowling EB (2002) Reactive nitrogen and the world: 200 years of change. Ambio 31:64–71. doi:10.1639/0044-7447(2002)031[0064:rnatwy]2.0.co;2

Galloway JN, Denterner FJ, Capone DG, Boyer EW, Howarth RW, Seitzinger SP, Asner GP, Cleveland CC, Green PA, Holland EA, Karl DM, Michaels AF, Porter JH, Townsend AR, Vorosmarty CJ (2004) Nitrogen cycles: past, present, and future. Biogeochemistry 70:153–226. doi:10.1007/s1 0533-004-0370-0

Galloway JN, Townsend AR, Erisman JW, Bekunda M, Cai ZC, Freney JR, Martinelli LA, Seitzinger SP, Sutton MA (2008) Transformation of the nitrogen cycle: recent trends, questions, and potential solutions. Science 320:889–892. doi:10.1126/science.1136674

Gong G, Mattevada S, O'Bryant SE (2014) Comparison of the accuracy of kriging and IDW interpolations in estimating groundwater arsenic concentrations in Texas. Environ Res 130:59–69. doi:10.1016/j.envres.2013.12.005

Goulding KWT (1990) Nitrogen deposition to land from the atmosphere. Soil Use Manag 6:61–63. doi:10.1111/j.1475-2743.1990.tb00801.x

Huang DY, Xu YG, Zhou B, Zhang HH, Lan JB (2010) Wet deposition of nitrogen and sulfur in Guangzhou, a subtropical area in South China Environ Monit Assess 171:429–439 doi:10.1007/s10661-009-1289-7

Huang J, Zhang W, Zhu X, Gilliam F, Chen H, Lu X, Mo J (2015) Urbanization in China changes the composition and main sources of wet inorganic nitrogen deposition. Environ Sci Pollut Res 22:6526–6534. doi:10.1007/s11356-014-3786-7

Huang YL, Lu XX, Chen K (2013) Wet atmospheric deposition of nitrogen: 20 years measurement in Shenzhen City, China. Environ Monit Assess 185:113–122. doi:10.1007/s10661-012-2537-9

Isaaks EH, Srivastava RM (1989) Applied geostatistics. Oxford University Press, New York, p. 561

Jia YL, Yu GR, He NP, Zhan XY, Fang HJ, Sheng WP, Zuo Y, Zhang DY, Wang QF (2014) Spatial and decadal variations in inorganic nitrogen wet deposition in China induced by human activity. Sci Rep 4:3763. doi:10.1038/srep03763

Journel AG, Kyriakidis PC, Mao S (2000) Correcting the smoothing effect of estimators: a spectral postprocessor. Math Geol 32:787–813

Kravchenko AN (2003) Influence of spatial structure on accuracy of interpolation methods. Soil Sci Soc Am J 67:1564–1571. doi:10.2136/sssaj2003.1564

Lü CQ, Tian HQ (2007) Spatial and temporal patterns of nitrogen deposition in China: synthesis of observational data. J Geophys Res Atmos 112. doi:10.1029/2006JD007990

Lü CQ, Tian HQ (2014) Half-century nitrogen deposition increase across China: a gridded time-series data set for regional environmental assessments. Atmos Environ 97:68–74. doi:10.1016/j.atmosenv.2014.07.061

Laslett GM, McBratney AB, Pahl PJ, Hutchinson MF (1987) Comparison of several spatial prediction methods for soil pH. J Soil Sci 38:325–341. doi:10.1111/j.1365-2389.1987.tb02148.x

Li J, Heap AD (2011) A review of comparative studies of spatial interpolation methods in environmental sciences: performance and impact factors. Ecol Infor 6:228–241. doi:10.1016/j.ecoinf.2010.12.003

Liu C, Wang Q, Zou C, Hayashi Y, Yasunari T (2015) Recent trends in nitrogen flows with urbanization in the Shanghai megacity and the effects on the water environment. Environ Sci Pollut Res 22:3431–3440. doi:10.1007/s11356-014-3825-4

Liu R, Chen Y, Sun C, Zhang P, Wang J, Yu W, Shen Z (2014) Uncertainty analysis of total phosphorus spatial-temporal variations in the Yangtze River Estuary using different interpolation methods. Mar Pollut Bull 86:68–75. doi:10.1016/j.marpolbul.2014.07.041

Liu XY, Xiao HY, Liu CQ, Li YY, Xiao HW (2008a) Stable carbon and nitrogen isotopes of the moss *Haplocladium microphyllum* in an urban and a background area (SW China): the role of environmental conditions and atmospheric nitrogen deposition. Atmos Environ 42:5413–5423. doi:10.1016/j.atmosenv.2008.02.038

Liu XY, Xiao HY, Liu CQ, Li YY, Xiao HW (2008b) Tissue N content and ^{15}N natural abundance in epilithic mosses for indicating atmospheric N deposition in the Guiyang area, SW China. Appl Geochem 23:2708–2715

Liu XJ, Duan L, Mo JM, Du EZ, Shen JL, Lu XK, Zhang Y, Zhou XB, He CE, Zhang FS (2011) Nitrogen deposition and its ecological impact in China: an overview. Environ Pollut 159:2251–2264. doi:10.1016/j.envpol.2010.08.002

Liu XY, Xiao HY, Liu CQ (2009) Quantification of atmospheric nitrogen deposition at Guiyang area based on nitrogen concentration of epilithic mosses. Acta Ecol Sin 29:6646–6653 (in Chinese)

Lloyd CD (2005) Assessing the effect of integrating elevation data into the estimation of monthly precipitation in Great Britain. J Hydrol 308:128–150. doi:10.1016/j.jhydrol.2004.10.026

Lu GY, Wong DW (2008) An adaptive inverse-distance weighting spatial interpolation technique. Comput Geosci 34:1044–1055. doi:10.1016/j.cageo.2007.07.010

Lu L, Cheng H, Pu X, Liu X, Cheng Q (2015) Nitrate behaviors and source apportionment in an aquatic system from a watershed with intensive agricultural activities. Environ Sci Proc Imp 17:131–144. doi:10.1039/C4EM00502C

Matheron G (1969) Le krigeage universel: cahiers du Centre de Morphologie Mathematique. Fontainebleau, Paris

Meyer M, Schröder W, Nickel S, Leblond S, Lindroos A-J, Mohr K, Poikolainen J, Santamaria JM, Skudnik M, Thöni L, Beudert B, Dieffenbach-Fries H, Schulte-Bisping H, Zechmeister HG (2015) Relevance of canopy drip for the accumulation of nitrogen in moss used as biomonitors for atmospheric nitrogen deposition in Europe. Sci Total Environ 538:600–610. doi:10.1016/j.scitotenv.2015.07.069

Mirzaei R, Sakizadeh M (2016) Comparison of interpolation methods for the estimation of groundwater contamination in Andimeshk-Shush Plain, southwest of Iran. Environ Sci Pollut Res 23:2758–2769. doi:10.1007/s11356-015-5507-2

Moran PAP (1948) The interpretation of statistical maps. J Royal Stat Soc Series B-Stat Method 10:243–251

Nadim F, Trahiotis MM, Stapcinskaite S, Perkins C, Carley RJ, Hoag GE, Yang X (2001) Estimation of wet, dry and bulk deposition of atmospheric nitrogen in Connecticut. J Environ Monit 3:671–680. doi:10.1039/B107008H

Nyberg F, Gustavsson P, Järup L, Bellander T, Berglind N, Jakobsson R, Pershagen G (2000) Urban air pollution and lung cancer in Stockholm. Epidemiology 11:487–495

Pan YP, Wang YS, Tang GQ, Wu D (2012) Wet and dry deposition of atmospheric nitrogen at ten sites in northern China. Atmos Chem Phys 12:6515–6535. doi:10.5194/acp-12-6515-2012

Pesch R, Schröder W, Schmidt G (2007) Nitrogen accumulation in forests. Exposure monitoring by mosses. Sci World J 7:151–158. doi:10.1100/tsw.2007.11

Pesch R, Schröder W, Schmidt G, Genssler L (2008) Monitoring nitrogen accumulation in mosses in central European forests. Environ Pollut 155:528–536. doi:10.1016/j.envpol.2008.02.018

Pitcairn C, Fowler D, Leith I, Sheppard L, Tang S, Sutton M, Famulari D (2006) Diagnostic indicators of elevated nitrogen deposition. Environ Pollut 144:941–950. doi:10.1016/j.envpol.2006.01.049

Pitcairn CER, Fowler D, Grace J (1995) Deposition of fixed atmospheric nitrogen and foliar nitrogen content of bryophytes and *Calluna vulgaris* (L.) Hull. Environ Pollut 88:193–205. doi:10.1016/0269-7491(95)91444-P

Pitcairn CER, Leith ID, Fowler D, Hargreaves KJ, Moghaddam M, Kennedy VH, Granat L (2001) Foliar nitrogen as an indicator of

nitrogen deposition and critical loads exceedance on a European scale. Water Air Soil Pollut 130:1037–1042. doi:10.1023/a:1013908312369

Pitcairn CER, Skiba UM, Sutton MA, Fowler D, Munro R, Kennedy V (2002) Defining the spatial impacts of poultry farm ammonia emissions on species composition of adjacent woodland ground flora using Ellenberg Nitrogen Index, nitrous oxide and nitric oxide emissions and foliar nitrogen as marker variables. Environ Pollut 119:9–21. doi:10.1016/S0269-7491(01)00148-8

Powell MJD (1990) The theory of radial basis function approximation in 1990. University of Cambridge Press, Cambridge

Schröder W, Holy M, Pesch R, Harmens H, Fagerli H, Alber R, Coskun M, De Temmerman L, Frolova M, González-Miqueo L, Jeran Z, Kubin E, Leblond S, Liiv S, Maňkovská B, Piispanen J, Santamaria P, Suchara I, Yurukova L, Thöni L, Zechmeister HG (2010) First Europe-wide correlation analysis identifying factors best explaining the total nitrogen concentration in mosses. Atmos Environ 44:3485–3491. doi:10.1016/j.atm os en v.2010.06.024

Schwartz J (1994) What are people dying of on high air pollution days? Environ Res 64:26–35. doi:10.1006/enrs.1994.1004

Skinner RA, Ineson P, Jones H, Sleep D, Leith ID, Sheppard LJ (2006) Heathland vegetation as a bio-monitor for nitrogen deposition and source attribution using $\delta^{15}N$ values. Atmos Environ 40:498–507. doi:10.1016/j.atmosenv.2005.09.054

Skudnik M, Jeran Z, Batič F, Kastelec D (2016) Spatial interpolation of N concentrations and $\delta^{15}N$ values in the moss *Hypnum cupressiforme* collected in the forests of Slovenia. Ecol Indic 61(Part 2):366–377. doi:10.1016/j.ecolind.2015.09.038

Skudnik M, Jeran Z, Batič F, Simončič P, Kastelec D (2015) Potential environmental factors that influence the nitrogen concentration and $\delta^{15}N$ values in the moss *Hypnum cupressiforme* collected inside and outside canopy drip lines. Environ Pollut 198:78–85. doi:10.1016/j.envpol.2014.12.032

Skudnik M, Jeran Z, Batič F, Simončič P, Lojen S, Kastelec D (2014) Influence of canopy drip on the indicative N, S and $\delta^{15}N$ content in moss *Hypnum cupressiforme*. Environ Pollut 190:27–35. doi:10.1016/j.envpol.2014.03.016

Solga A, Burkhardt J, Zechmeister HG, Frahm JP (2005) Nitrogen content, 15 N natural abundance and biomass of the two pleurocarpous mosses *Pleurozium schreberi* (Brid.) Mitt. and Scleropodium purum (Hedw.) Limpr. in relation to atmospheric nitrogen deposition. Environ Pollut 134:465–473. doi:10.1016/j.envpol.2004.09.008

Stahl K, Moore RD, Floyer JA, Asplin MG, McKendry IG (2006) Comparison of approaches for spatial interpolation of daily air temperature in a large region with complex topography and highly variable station density. Agric For Meteorol 139:224–236. doi:10.1016/j.agrformet.2006.07.004

Stone M (1974) Cross-validatory choice and assessment of statistical predictions. J Royal Stat Soc Series B—Stat Method 36:111–147

Sun Y, Kang S, Li F, Zhang L (2009) Comparison of interpolation methods for depth to groundwater and its temporal and spatial variations in the Minqin oasis of northwest China. Environ Model Softw 24:1163–1170. doi:10.1016/j.envsoft.2009.03.009

Varela Z, Carballeira A, Fernández JA, Aboal JR (2013) On the use of epigaeic mosses to biomonitor atmospheric deposition of nitrogen. Arch Environ Contam Toxicol 64:562–572. doi:10.1007/s00244-012-9866-0

Wagner PD, Fiener P, Wilken F, Kumar S, Schneider K (2012) Comparison and evaluation of spatial interpolation schemes for daily rainfall in data scarce regions. J Hydrol 464-465:–400. doi:10.1016/j.jhydrol.2012.07.026

Weber D, Englund E (1992) Evaluation and comparison of spatial interpolators. Math Geol 24:381–391. doi:10.1007/BF00891270

Wu X, Yan L (2007) Setting parameters and choosing optimum semivariogram models of ordinaty kriging interpolation—a case study of spatial interpolation to January average temperature of Fujian province. Geo-Inform Sci 9:104–108 (in Chinese)

Xiao HY, Tang CG, Xiao HW, Liu XY, Liu CQ (2010a) Stable sulphur and nitrogen isotopes of the moss *Haplocladium microphyllum* at urban, rural and forested sites. Atmos Environ 44:4312–4317. doi:10.1016/j.atmosenv.2010.05.023

Xiao HY, Tang CG, Xiao HW, Liu XY, Liu CQ (2010b) Mosses indicating atmospheric nitrogen deposition and sources in the Yangtze River Drainage Basin, China. J Geophys Res Atmos (1984a) 115. doi:10.1029/2009JD012900

Xiao HY, Xie ZY, Tang CG, Wang YL, Liu CQ (2011) Epilithic moss as a bio-monitor of atmospheric N deposition in South China. J Geophys Res Atmos (1984b) 116. doi:10.1029/2011JD016229

Xie Y, Chen TB, Lei M, Yang J, Guo QJ, Song B, Zhou XY (2011) Spatial distribution of soil heavy metal pollution estimated by different interpolation methods: accuracy and uncertainty analysis. Chemosphere 82:468–476. doi:10.1016/j.chemosphere.2010.09.053

Yao X, Fu B, Lu Y, Sun F, Wang S, Liu M (2013) Comparison of four spatial interpolation methods for estimating soil moisture in a complex terrain catchment. Plos One 8. doi:10.1371/journal.pone.0054660

Zhang YQ, Chen CC, Yin YX, Yang XH (2013) Spatial interpolation model selection of multi-year average precipitation in Jiangxi Province. Res Soil Water Conserv 20:69–74 (in Chinese)

Zhong JL (2010) Study on spatial precipitation interpolation precision based on GIS in Xinjiang. Arid Environ Monitor 24:43–46 (in Chinese)

Zhu JX, He NP, Wang QF, Yuan GF, Wen D, Yu GR, Jia YL (2015) The composition, spatial patterns, and influencing factors of atmospheric wet nitrogen deposition in Chinese terrestrial ecosystems. Sci Total Environ 511:777–785. doi:10.1016/j.scitotenv.2014.12.038

Zimmerman D, Pavlik C, Ruggles A, Armstrong M (1999) An experimental comparison of ordinary and universal kriging and inverse distance weighting. Math Geol 31:375–390. doi:10.1023/A:1007586507433